Supplementary Information

Far-field Imaging of Non-fluorescent Species with Sub-diffraction Resolution

Pu Wang et al.

Theory of saturated transient absorption microscopy

Based on the theoretical interpretation on the saturation mechanism of graphene [1], the signal in saturated transient absorption microscopy is estimated as follows. The optical transmission of probe radiation through graphene as a function of the power of pump radiation in the near infrared and visible region can be approximated as [1]:

$$T_{Pr} \approx T_0 + \frac{hI_p}{1+I_p/I_0}, \quad \text{(S1)}$$

where T_{pr} is the transmission of the probe beam, T_0 is the transmission of the probe beam without the presence of pump, I_p is the power density of the pump beam, h and I_0 are constants representing the modulation transfer coefficient and the power density for saturated absorption, respectively. The contrast of a pump-probe measurement comes from the difference probe transmission between the pump field on and off states, and can be derived from eq. (S1) as

$$\Delta T_{pr} = \frac{hI_p}{1+I_p/I_0}. \quad \text{(S2)}$$

When adding the un-modulated saturation beam, $I_{sat,}$ the pump-probe signal becomes

$$\Delta T'_{pr} = \frac{h(I_p+I_{sat})}{1+(I_p+I_{sat})/I_0} - \frac{hI_{sat}}{1+I_{sat}/I_0}, \quad \text{(S3)}$$

where I_{sat} is the peak power density of the saturation beam. Considering $I_p << I_0$, the signal of a pump-probe measurement is linear to the pump power and eq. (S3) becomes

$$\Delta T_{pr} = \frac{hI_p}{1+I_{sat}/I_0}. \quad \text{(S4)}$$

Eq. (S4) indicates that the pump-probe signal is suppressed in the presence of a high intensity saturation beam and it drops to half when $I_{sat} = I_0$.

Effective point spread function for pump-probe microscopy in diffraction-limited condition

The resolution of the image is determined by the effective point spread function (PSF) of the excitation volume, the PSF of the detection system and the size of the object. Given the nonlinear nature of the pump-probe technology and aperture free detection, the effective image formation under microscope is described by:

$$P_{(x,y)} \propto PSF_{eff} \otimes O_{(x,y)} \quad \text{(S5)}$$

where PSF_{eff} is the effective PSF of the illumination lasers, $O_{(x,y)}$ is the object function. $\otimes$ denotes the convolution operator. Because pump probe microscopy is a nonlinear optical measurement, where the heterodyne-detected signal $\Delta I_{pr} = \sigma I_p I_{pr}$, the effective PSF equals $PSF_{pump} \times PSF_{probe}$. If the Airy disk is approximated by a Gaussian function, the effective PSF is described as:

$$I_{eff}(r) \approx I_p e^{\frac{-2r^2}{w_p{}^2}} \times I_{pr} e^{\frac{-2r^2}{w_{pr}{}^2}}, \quad \text{(S6)}$$

where r is the radial distance from the center of the Airy disk. w_p and w_{pr} are the Gaussian width of the two beams, which can be approximated as $0.45\lambda_p$/N.A. and $0.45\lambda_{pr}$/N.A., respectively. From **eq. S6,** the effective PSF can be represented by a Gaussian function with the Gaussian

width of $\sqrt{1/(\frac{1}{{w_p}^2}+\frac{1}{{w_{pr}}^2})}$. As FWHM of a Gaussian function can be calculated to be $2\sqrt{ln2}w$, the effective FWHM can be estimated as:

$$FWHM_{eff} = \frac{0.53}{N.A.}\sqrt{(1/(\frac{1}{{\lambda_p}^2}+\frac{1}{{\lambda_{pr}}^2})} \ . \qquad \text{(S7)}$$

Taking into consideration the nonlinearity of the high N.A. = 1.2 objective used in this work, the full-width at half-maximum (FWHM) of the diffraction-limited effective PSF could be a little higher [2,3]. The resulting FWHM of the effective PSF under diffraction-limited condition is calculated to be ~300 nm.

PSF and lateral spatial resolution of saturated transient absorption microscopy

With the presence of the saturation beam engineered to a doughnut shape at the focus, the same theory used in stimulated emission depletion microscopy and ground state depletion microscopy [4] is applicable to estimate the FWHM of the effective PSF of the probe beam:

$$FWHM'_{pr} \approx \lambda_{pr}/[2(N.A.)\sqrt{1+I_{sat}/I_0}]. \qquad \text{(S9)}$$

If the effective PSF of the probe is approximated as a Gaussian function, the effective PSF of the system is given by:

$$I_{eff}(r) = I_p e^{\frac{-2r^2}{{wp}^2}} \times I'_{pr} e^{\frac{-2r^2}{{w'_{pr}}^2}}, \qquad \text{(S10)}$$

where $w'_{pr} = FWHM'_{pr}/2\sqrt{ln2}$. The FWHM of the effective PSF is then estimated by:

$$FWHM_{eff} \approx \frac{1}{2N.A.}\sqrt{1/(\frac{1}{{\lambda_{pr}}^2/(1+I_{sat}/I_0)}+\frac{1}{{\lambda_p}^2})}. \qquad \text{(S11)}$$

Based on the fitting result from Fig. 3 (d) and the parameters we used in the saturated transient absorption imaging experiment, we expected a FWHM of the effective PSF to be ~160 nm.

The experimentally measured resolution of saturated transient absorption microscopy

We evaluated the FWHM in multiple platelets (light blue circle in **Fig. S1(A)**) along various angles (0, 45, 90, 135 degree). The averaged FWHMs for each nano-platelet are 260 ± 36 nm, 248 ± 23 nm, 249 ± 29 nm, 241 ± 16 nm, 233 ± 51 nm, 232 ± 25 nm, 238 ± 27 nm, 250 ± 29 nm, 259 ± 45 nm, 283 ± 12 nm, respectively. The total averaged FWHM is 249 ± 31 nm. FWHMs of the nano-platelets as a function of the line angle are shown in **Fig. S1(B)**. The measured averaged FWHM has maximum at 45 degree angle. However it is within standard deviation from results for other angles.

Characterization of the graphene and graphite nano-platelets sample

Pump-probe images and Raman spectra of graphene and graphite nano-platelets were recorded using a multimodal microscope described in [5]. Briefly, two electronically synchronized Ti:sapphire lasers at 885 nm and 707 nm with 5 ps pulse duration was applied as pump and probe, respectively. Confocal Raman micro-spectroscopy was performed at the point of interest, using the 707 nm beam as the excitation source.

References

1 Vasko, F. T. Saturation of interband absorption in graphene. *Phys. Rev. B* **82**, 245422 (2010).

2 Zipfel, W. R., Williams, R. M. & Webb, W. W. Nonlinear magic: multiphoton microscopy in the biosciences. *Nat. Biotechnol.* **21**, 1369-1377 (2003).

3 Sheppard, G. J. R. & Matthews, H. J. Imaging in high-aperture optical systems. *J. Opt. Soc. Am. A* **4**, 1354-1360 (1987).

4 Hell, S. W. Toward fluorescence nanoscopy. *Nat. Biotechnol.* **21**, 1347-1355 (2003).

5 Slipchenko, M. N., Le, T. T., Chen, H. & Cheng, J.-X. High-Speed Vibrational Imaging and Spectral Analysis of Lipid Bodies by Compound Raman Microscopy. *J. Phys. Chem. B* **113**, 7681-7686 (2009).

Supplementary Figure 1

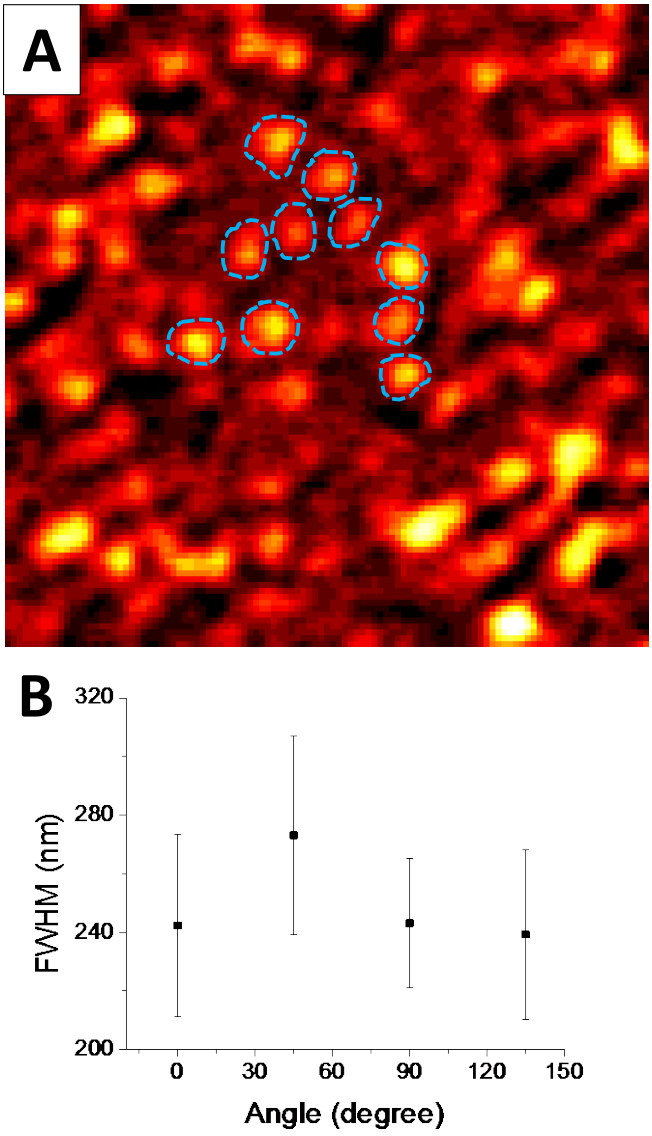

Figure S1. **Experimental evaluation of the resolution of saturated transient absorption microscopy.** (A) Selected nano-platelets for FWHM measurements. (B) FWHMs measured as function of angle with respect to the vertical axis.

Supplementary Figure 2

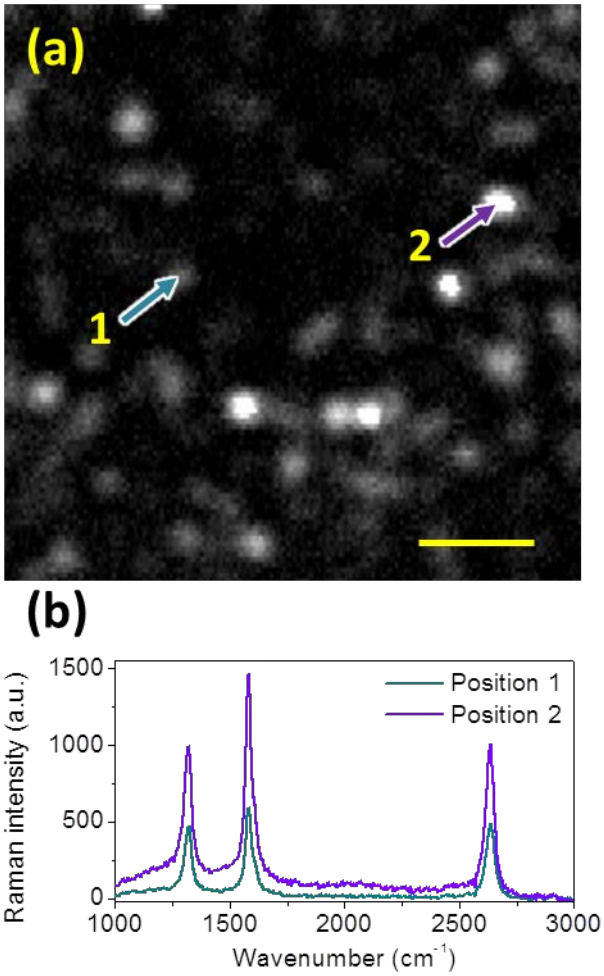

Figure S2. Pump-probe image (a) and Raman spectra (b) of graphite nano-platelets. The Raman spectra were taken at the indicated spots in (a). Scale bar: 2 μm

Supplementary Figure 3

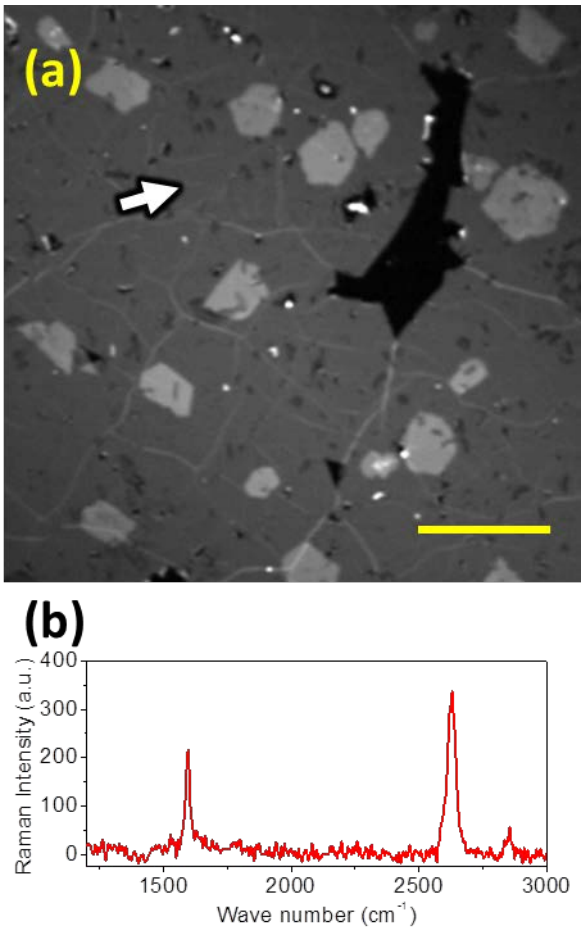

Figure S3. Pump-probe image (a) and Raman spectrum (b) of graphene. The Raman spectrum was taken at the indicated spot in (a). Scale bar: 20 μm